# Recombinant human angiotensin-converting enzyme 2 plays a protective role in mice with sepsis-induced cardiac dysfunction through multiple signaling pathways dependent on converting angiotensin II to angiotensin 1–7

**Chunxue Wu[1,2,3], Yuhong Chen[1,3], Pan Zhou[1,3], Zhenjie Hu[1,3]**

[1]Department of Critical Care Medicine, The Fourth Hospital of Hebei Medical University, Shijiazhuang, China; [2]Intensive Care Unit of Emergency Department, Neurology Branch of Cangzhou Central Hospital, Cangzhou, China; [3]Hebei Key Laboratory of Critical Disease Mechanism and Intervention, Shijiazhuang, China

*Contributions:* (I) Conception and design: Z Hu, Y Chen, C Wu; (II) Administrative support: Z Hu; (III) Provision of study materials or patients: Z Hu, Y Chen, C Wu; (IV) Collection and assembly of data: C Wu, P Zhou; (V) Data analysis and interpretation: C Wu, Y Chen; (VI) Manuscript writing: All authors; (VII) Final approval of manuscript: All authors.

*Correspondence to:* Zhenjie Hu. Department of Critical Care Medicine, The Fourth Hospital of Hebei Medical University, 12 Jiankang Road, Shijiazhuang 050011, China. Email: syicuhzj@163.com.

**Background:** Sepsis-induced cardiac dysfunction (SICD) is a common complication of sepsis and contributes to mortality and the complexity of management in patients with sepsis. Recombinant human angiotensin-converting enzyme 2 (rhACE2) has been reported to protect the heart from injury and dysfunction in conditions which involve increased angiotensin II (Ang II). In this study, we aimed to detect the effects of rhACE2 on SICD.

**Methods:** A SICD model was developed in male C57/B6 mice by lipopolysaccharide (LPS) intraperitoneal injection. When cardiac dysfunction was confirmed by echocardiography 3 hours after LPS administration, mice were treated with either saline, rhACE2, or rhACE2 + A779. All mice received echocardiographic examination at 6 hours after LPS injection and then were sacrificed for serum and myocardial tissues collection. Angiotensin, cardiac troponin I (cTnI), and inflammatory markers in serum were measured. Histopathology features were examined by hematoxylin and eosin (HE) and terminal deoxynucleotidyl transferase (TdT) dUTP nick-end labeling (TUNEL) staining to evaluate structure injury and cell pyroptosis rate in heart tissue respectively. Pyroptosis-related proteins and signaling pathways involved in nucleotide binding and oligomerization domain-like receptor family pyrin domain-containing 3 (NLRP3) inflammasome activation in heart tissue were investigated by western blot (WB).

**Results:** RhACE2 relieved myocardial injury and improved cardiac function in mice with SICD accompanied by decrease of Ang II and increase of angiotensin 1–7 (Ang 1–7) in serum. RhACE2 diminished activation of NLRP3 inflammasome, inflammatory response, and cell pyroptosis induced by LPS. In addition, rhACE2 partly inhibited activation of nuclear factor κB (NF-κB), the p38 mitogen-activated protein kinase (MAPK) pathway, and promoted activation of the AMP-activated protein kinase-α1 (AMPK-α1) pathway in heart tissue. Administration of A779 offset the inhibitive effects of rhACE2 on NLRP3 expression and protective role on cardiac injury and dysfunction in mice with SICD.

**Conclusions:** RhACE2 plays a protective role in SICD, ameliorating cardiac injury and dysfunction through NF-κB, p38 MAPK, and the AMPK-α1/NLRP3 inflammasome pathway dependent on converting Ang II to Ang 1–7.

**Keywords:** Angiotensin-converting enzyme 2 (ACE2); angiotensin II (Ang II); heart disease; lipopolysaccharide (LPS); sepsis

Submitted Oct 31, 2022. Accepted for publication Dec 29, 2022. Published online Jan 10, 2023.
doi: 10.21037/atm-22-6016
**View this article at:** https://dx.doi.org/10.21037/atm-22-6016

## Introduction

Sepsis is a life-threatening syndrome caused by the host's dysregulated immune response to infection, which consecutively causes organ dysfunction, disability, and even death (1). Evidence accumulated over the past decades shows a high incidence of sepsis, especially in the intensive care unit (ICU) all over the world (2-5). Though the understanding and management of sepsis have been improving during the past years, the reported mortality remains as high as 20–40% (2,4,6,7).

Sepsis-induced cardiac dysfunction (SICD) is a common complication that exacerbates the poor prognosis of patients, most of which is characterized by reduced left ventricular ejection fraction (LVEF) and diminished contractility (8). In patients with SICD, the mortality is increased 2–3 times (9), which is reported as approximately 70–90% (10). Precise mechanisms and effective therapy in patients with SICD remain unclear and need further exploration to improve its management and outcomes.

The renin-angiotensin-aldosterone system (RAAS) includes classic pathway in which angiotensin II (Ang II) is the main effector and non-classic RAAS pathway in which angiotensin 1–7 (Ang 1–7) plays the key role. Both pathways are expressed in various cells in heart including cardiomyocytes, fibroblasts, endothelia, and immune cells (11-14). Ang II is known to promote heart failure through inducing cardiac hypertrophy, fibrosis, and ventricular remodeling depending on its pro-inflammatory effects (15,16). On the contrary, the non-classic RAAS in heart exerts a cardiac protective role opposite to Ang II (17). Angiotensin-converting enzyme 2 (ACE2), which can inactivate Ang II by catalyzing it to Ang 1–7 (18) shows cardiac beneficial effects depending on its cleavage action of Ang II (19,20).

Evidences indicated that Ang II is enhanced in sepsis and involved in the pathophysiology of organ injury (21,22). Ang II leads to an up-regulation of pro-inflammatory cytokines such as tumor necrosis factor-α (TNF-α) and interleukin-1 (IL-1) and subsequent macrophage infiltration, microvascular ischemia, and cardiac dysfunction in sepsis (23). Treatment targeted to balance the disturbed RAAS in septic animal models show anti-inflammatory effects and are beneficial to heart function and survival (24).

ACE2, which is a homolog of ACE1, is a negative regulator of RAAS by converting Ang II to Ang 1–7 (15). A recombinant human ACE2 (rhACE2; APN01, GSK2586881) has been found to have protective effects on cardiac dysfunction and injury in both inflammatory and non-inflammatory cardiac injury models and to be safe, with no negative hemodynamic effects in healthy volunteers and in patients with acute respiratory distress syndrome (ARDS) (25,26).

The nucleotide binding and oligomerization domain-like receptor family pyrin domain-containing 3 (NLRP3) inflammasome, which consists of 3 members, namely apoptosis-associated speck-like protein (ASC), NLRP3, and pro-caspase-1 (27), is a vital mediator pathway of the innate immune system and has recently gained close attention in SICD research.

Previous studies have shown that NLRP3 inflammasome triggers the cardiomyopathy of polymicrobial sepsis induced by cecal ligation and puncture (CLP) (28) and Ang II is

### Highlight box

**Key findings**

- RhACE2 played a protective role in SICD through multiple pathways depending on converting Ang II to Ang 1–7.

**What is known and what is new?**

- Modulating changes of angiotensin contributes to improving cardiac function in non-septic conditions, such as hypertension and diabetes mellitus. RAAS is activated during sepsis and NLRP3 is involved in the development of SICD.
- Depending on converting Ang II to Ang 1–7, RhACE2 alleviated cardiac injury and improved heart function in a septic model through NLRP3 related pathways.

**What is the implication, and what should change now?**

- Modulating changes of angiotensin could be a new idea for managing SICD, and well-designed studies are needed to explore the precise mechanisms and treatments of SICD.

involved in nuclear factor κB (NF-κB)-mediated NLRP3 inflammasome activation (29). Therefore, we hypothesized that regulating NLRP3 inflammasome through modulating the activation of RAAS may play a protective role in mice with SICD.

Lipopolysaccharide (LPS) is widely accepted to be used *in vivo* and *in vitro* to simulate the clinical conditions of sepsis and SICD for years (30,31). By intraperitoneal injection to mouse, we can get a mouse model of SICD easily and economically.

In our study, we built a model of LPS-induced cardiac dysfunction with mouse to investigate the effects of rhACE2 on SICD and the probable mechanism of it. We present the following article in accordance with the ARRIVE reporting checklist (available at https://atm.amegroups.com/article/view/10.21037/atm-22-6016/rc).

## Methods

### *Animals and treatment*

Male healthy C57/B6 mice (animal certification No. 110011210104951884) aged 8–10-week, and weighing 20–25 g, were purchased from Vital River Laboratories, Beijing, China. Before initiating the experiment, a week of acclimation was allowed. The animal was housed in standard pathogen-free environment (22 ℃, light/dark cycle of 12/12 h) with enough standard food and water. A protocol was prepared before the study without registration. The investigator (PZ) in charge of group allocation was the only person who know the group allocation in our team. The study was approved by the laboratory animal ethical committee of Animal Experiment Center of the Fourth Hospital of Hebei Medical University (No. 2020002). Hebei Key Laboratory of Critical Disease Mechanism and Intervention was informed and agreed with this study. All procedures were conducted in the Animal Experiment Center of the institute above and Hebei Key Laboratory of Critical Disease Mechanism and Intervention, in accordance with the Guide for the Care and Use of Laboratory Animals of Institutes of Health (Eighth Edition).

The SICD model was established via intraperitoneal LPS injection. According to the previous work of our team, we obtained 60% of mice with significant myocardial dysfunction at 3 hours after intraperitoneal LPS injection and significance of outcome measures among groups, each of which contained 6 mice (32). The experiment was carried out in two parts. In the first part, the control, LPS, and LPS + rhACE2 groups were arranged to investigate the effects of rhACE2 on mice with LPS-induced cardiac dysfunction. In detail, following the table of random digit, 6 mice were distributed to the control group and at least 20 mice were allocated to a model-establish group that would be subsequently randomly assigned to a LPS group and a LPS + rhACE2 group (6 per group). Mice in the model-establish group were injected with LPS (10 mg/kg, *Escherichia coli* 055:B5, Cat. No. L8880, Solarbio, Beijing, China) intraperitoneally, and mice in the control group were intraperitoneally injected with an isovolumetric saline. Mice that were injected with LPS yet showed no significant decrease of LVEF and left ventricular fractional shortening (LVFS) at 3 hours after LPS administration compared to the control group were excluded and euthanized by cervical dislocation to reduce their suffering. The LPS-injected mice that displayed a significant decrease of LVEF and LVFS at 3 hours after LPS administration were included and allocated to either LPS group or LPS + rhACE2 group according to the random number method. RhACE2 (Cat No. HY-P7442, MedChemExpress, USA) was dissolved in normal saline 0.9% and intraperitoneally injected at a dose of 200 μg/kg (25,33) into mice allocated to the LPS + rhACE2 group immediately after group allocation. The remaining mice were treated with isovolumetric saline. All mice underwent echocardiographic re-evaluation at 6 hours after LPS injection and were sacrificed rapidly by cervical dislocation. Inhaling isoflurane (2%) anesthesia was applied to all mice to reduce their suffering during echocardiographic examination. The blood and myocardial tissues were collected. To minimize the influence of the order of treatments and measurements on the outcome, we applied the treatment, echocardiographic examination, and sample collection in the same order. The serum samples were isolated through centrifugation (3,000 rpm, 15 minutes) at 4 ℃ and frozen at −80 ℃ immediately. The heart samples were rinsed with phosphate-buffered saline (PBS) to remove the residual blood and frozen at −80 ℃ for further investigation.

A779, a selective mas receptor antagonist of Ang 1–7, was used to further elucidate the mechanism of the effects of rhACE2 on LPS-induced cardiac dysfunction in the second part. In detail, four groups (the control group, the LPS group, LPS + rhACE2 group, and LPS + rhACE2 group +A779, each containing 6 mice), were used to investigate the LVEF and LVFS, cardiac structure injury, pyroptosis cell rates, and NLRP3 expression in heart tissue. The establishment of the SICD model, and the criteria

of inclusion and exclusion were same to those of the first part. Random numbers were also used for group allocation. Besides the LPS group and LPS + rhACE2 group, mice with LPS-induced cardiac dysfunction were also distributed randomly to the LPS + rhACE2 +A779 group, receiving 10 mg/kg A779, (HY-P0216, MedChemExpress, Monmouth Junction, NJ, USA) by tail vein injection (34) prior to receiving 200 μg/kg rhACE2 by intraperitoneal injection. All the mice were also sacrificed after cardiac function evaluation by echocardiography at 6-hour after LPS treatment under inhaling isoflurane anesthesia. The serum samples and myocardial tissues were collected as described previously.

### *Echocardiography*

LVEF and LVFS were obtained from M-mode detection of left ventricular (LV) to evaluate cardiac function of mice by a special ultrasound instrument (Vevo 2100 imaging system, VisualSonics, Ontario, Canada) for small animals with a 13-MHz linear transducer under isoflurane inhalation anesthesia. The sonographer was blinded to the group allocation.

### *Indicators of myocardial injury and inflammation*

Commercial enzyme-linked immunosorbent assay (ELISA) kits were obtained to examine the serum levels of indicators myocardial injury and inflammation. Cardiac troponin I (cTnI; Cat No. E-EL-M1203c, Elabscience Biotechnology, Wuhan, China) was the indicator of cardiac injury we used. The inflammatory factors included TNF-α (Cat No. KE10002, Proteintech, Wuhan, China), IL-18 (Cat No. CSB-E04609m, CUSABIO, Wuhan, China), and IL-1β (Cat No. KE10003, Proteintech).

### *Angiotensin in serum*

Serum concentrations of Ang II (Cat No. CSB-E04495m, CUSABIO) and Ang 1–7 (Cat No. CSB-E13763m, CUSABIO) were investigated through ELISA kits on the basis of the manufacturer's instructions.

### *Hematoxylin and eosin (HE) staining*

Myocardial tissues were fixed in 4% paraformaldehyde for over 24 hours, embedded in paraffin, cut into 4 μm-thick sections, and stained with HE at room temperature. Two skilled pathologists who were blind to the interventions examined the extent of myocardial injury with a light microscope (DM3000 LED, Leica, Wetzlar, Germany) at 200× magnification and photographed them with a digital camera. The extent of myocardial injury showed in sections were scored using a semi-quantitative method as previously described: 0 for no damage; 1 for damage involving no more than 25% of the myocardium and 2 for 25–50%, 3 for 50–75%, and 4 for 75%, respectively (35,36). The average score of two sections of each sample were used for analysis.

### *Terminal deoxynucleotidyl transferase (TdT) dUTP nick-end labeling (TUNEL) staining*

TUNEL staining was performed to identify pyroptosis cells in heart tissue sections with a TUNEL assay kit (Servicebio, G1501, Wuhan, China). Myocardial tissue sections were deparaffinized with xylene and rehydrated with ethanol, and then were reacted with proteinase K working solution (Servicebio, G1205) at 37 ℃ for 25 minutes and completely washed with PBS. Sections were further incubated with permeabilize working solution (the membrane breaking fluid was 0.1% triton. Configuration method, triton stock solution:PBS =1:1,000) for 20 minutes and washed. TUNEL staining was performed following the manufacturer's protocol. Microscopic examination was performed, and images were collected through a fluorescence microscope (Nikon, Tokyo, Japan). Cells that were positively labeled (green) were quantified in 10 different fields per slide by Image J software (1.53a, Wayne Rasband, NIH, USA). The means and standard deviations (SDs) were derived from counting a minimum of three fields from two different coverslips per sample.

### *Western blot (WB) analysis*

According to the instructions, whole proteins were extracted from heart tissues in radioimmunoprecipitation assay (RIPA) buffer (P0013B, Beyotime, Nanjing, China) with phosphatase inhibitor in it. The protein content was measured with a bicinchoninic acid (BCA) kit (Cat No. SW101-02, SEVEN, Beijing, China). Protein samples (40 μg per lane) were separated by 8% or 12% sodium dodecyl sulfate polyacrylamide gel electrophoresis (SDS-PAGE) gels and then transferred onto polyvinylidene fluoride (PVDF) membranes (Millipore-Upstate, Beijing, China, 0.45 or 0.22 μm). Nonfat milk (Cat No.

1172GR500, Saiguo, Guangzhou, China) or albumin (Solarbio) resolved in tris-buffered saline solution with 0.1% Tween-20 (TBST) were used to block the membranes (37 ℃ for 2 hours). Membranes were then incubated at 4 ℃ overnight with primary antibodies against {[NLRP3 1:1,000, anti-NLRP3 antibody (EPR23094-1), Cat No. ab263899, Abcam, Cambridge, UK], gasdermin D [GSDMD; 1:1,000, anti-GSDMD (EPR19828), Cat No. ab209845, Abcam], caspase-1 [1:1,000, Cat No. ab179515, anti-pro-caspase-1 + p10 + p12 antibody (EPR 16883), Abcam], NF-κB (1:500, NF-κB p65 Ab, Cat No. AF 5006, Affinity Biosciences, Liyang, China), p-NF-κB [1:500, phospho-NF-κB p65 (Ser536) Ab, Cat No. AF 2006, Affinity Biosciences], AMP-activated protein kinase (AMPK; 1:500 catalog number 10929-2-AP AMPK alpha 1 rabbit polyclonal antibody, Proteintech), p-AMPK [1:500; phospho-AMPK (Thr172) (D4D6D), Cat No. #50081, Cell Signaling Technology, Danvers, MA, USA], p38 mitogen-activated protein kinase (MAPK; 1:500, p38 MAPK rabbit polyclonal antibody, Cat No. 14064-1-AP, Proteintech), p-P38 MAPK [1:500, phosph-p38 MAPK Thr180/Tyr182(D3F9)XP Rabbit mAb, Cat No. #4511, Cell Signaling Technology], and α-tubulin (alpha tubulin rabbit polyclonal antibody 1:5,000, Cat No. 11224-1-AP, Proteintech)}. The membranes were washed in TBST 3 times (15 minutes each time) followed by incubation with HRP-linked secondary antibodies (1:10,000, Cat No. SA00001-2, Proteintech) (room temperature for 2 hours). Enhanced chemiluminescence (ECL) detection kit (Cat No. P10300, NcmBiotech, Suzhou, China) and BLT GelView 6000Plus (Fluorchem E, Santa Clara, CA, USA) were used to visulize the protein bands. Image J software (1.53a, Wayne Rasband) was used to quantify the intensities of the bands. Alpha-tubulin was used as internal control.

### *Statistical analyses*

The results were represented as mean ± SD and analyzed using Graph Prism 8.0 (GraphPad Software, San Diego, CA, USA) and SPSS 26.0 software (IBM Corp., Armonk, NY, USA). The differences between the two groups were compared by Student's unpaired *t*-test. Differences among multiple groups were analyzed by one-way analysis of variance (ANOVA) followed by a post hoc analysis by least significance difference (LSD) test or Tamhane's T2 test, depending on the deference of variances. Correlation between serum levels of Ang II and levels of NLRP3 expression in heart tissue was analyzed by Pearson correlation analysis. Statistical significance was regarded as $P<0.05$.

## Results

### *RhACE2 improved cardiac function in mice with LPS-induced cardiac dysfunction*

In the first section of the study, 18 (6 per group) out of the total 28 mice that were enrolled completed the experiment. Due to absence of significant decline in LVEF and LVFS, 10 mice were excluded. Manifestation of the animal received LPS injection included lethargy, mild closure of the eyes, ruffled fur, and diarrhea consistent to those of endotoxemia. All mice among groups weighed comparably and survived at 6 hours after intervention. LVEF and LVFS of mice at 3 hours after LPS injection in the LPS group and LPS + rhACE2 group were significantly lower than those in control group. Compared with the LPS group, LVEF and LVFS improved significantly in the LPS + rhACE2 group at 3 hours after rhACE2 treatment (*Figure 1A-1C*).

### *RhACE2 administration relieved myocardial injury in mice with LPS-induced cardiac dysfunction*

The HE staining of myocardial sections indicated widespread myocardial structure disorder, interstitial hemorrhage and edema, and infiltration with neutrophil granulocytes in LPS-induced cardiac dysfunction mice, which were relieved significantly by rhACE2 treatment in the LPS + rhACE2 group (*Figure 2A,2B*). Compared with the control group, cTnI concentration in serum increased significantly at 6 hours in the LPS group. Compared with the LPS group, cTnI concentration in serum in the LPS + rhACE2 group decreased significantly (*Figure 2C*).

### *RhACE2 significantly inhibited activation of NLRP3 inflammasome followed by significant decrease of NLRP3 inflammasome-related inflammatory factors in serum and cell pyroptosis in heart tissues induced by LPS*

According to WB analysis of heart tissue, expression of NLRP3 in the LPS group were significantly higher than those in control group, and expression of NLRP3 in the LPS + rhACE2 group was significantly lower than that in the LPS group. Expressions of the other two classic pyroptosis-associated proteins, N-terminal cleavage product of GSDMD (GSDMD-NT) and caspase-1 p12 (cleavage product of caspase-1 p46) in heart tissues were

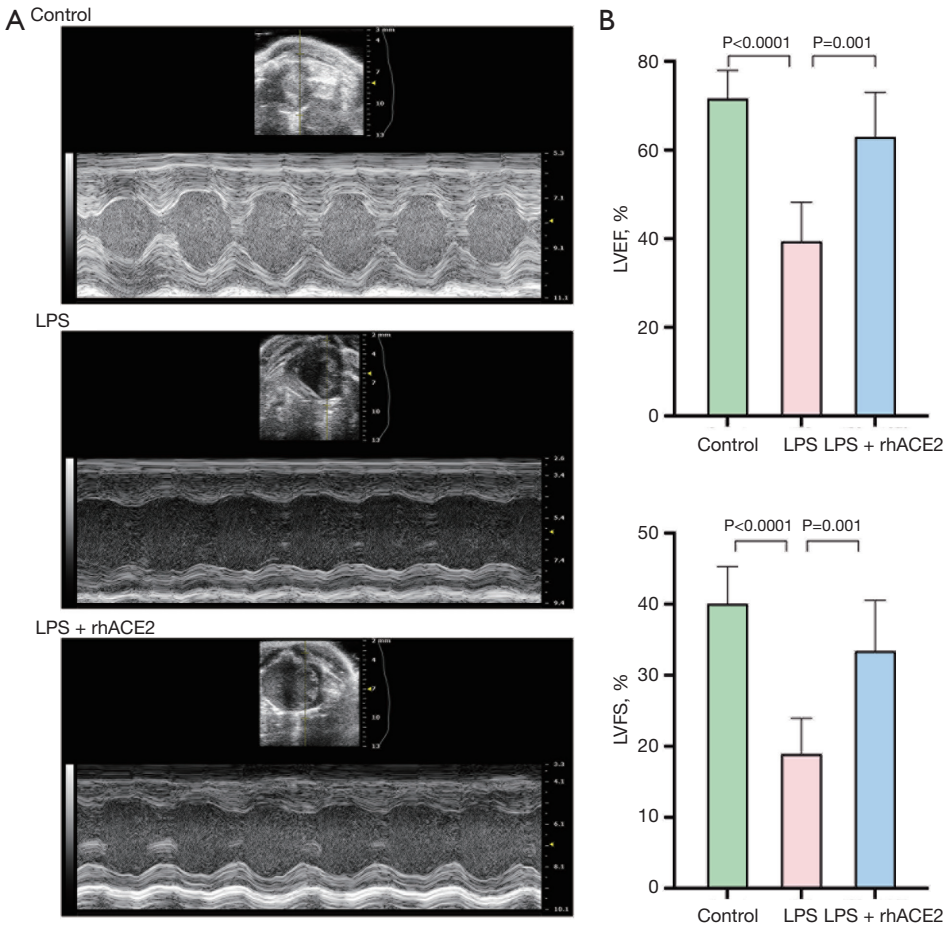


**Figure 1** RhACE2 administration improves cardiac function in mice with LPS-induced cardiac dysfunction. (A) Transthoracic echocardiography (M-mode) of mice among three groups (6 per group). (B,C) Comparison of LVEF and LVFS of mice among three groups (6 per group). Data are expressed as mean ± SD. LPS, lipopolysaccharide; rhACE2, recombinant human angiotensin-converting enzyme 2; LVEF, left ventricular ejection fraction; LVFS, left ventricular fractional shortening; SD, standard deviation.

also increased in the LPS group and then decreased after rhACE2 treatment (*Figure 3A-3D*). Serum concentrations of IL-1β and IL-18, the inflammatory factors matured through NLRP3 inflammasome activation, increased significantly in the LPS group and decreased significantly under the treatment of rhACE2 (*Figure 3E,3F*). And the significant increase in serum of TNF-α, the representative inflammatory factor in sepsis, was also suppressed by rhACE2 (*Figure 3G*). TUNEL staining of heart tissue sections showed that pyroptosis cell rates in the LPS group significantly increased compared with those in control group, and decreased significantly in the LPS + rhACE2 group compared with those in LPS group (*Figure 3H,3I*).

### *RhACE2 regulated changes of angiotensin in LPS-induced cardiac dysfunction mice, and the levels of Ang II in serum had a significantly positive correlation with levels of NLRP3 expression in heart tissue*

In the LPS group, Ang II and Ang 1–7 levels in serum were significantly higher than those in the control group. Compared with the LPS group, levels of Ang II in serum decreased significantly in the LPS + rhACE2 group, and levels of Ang 1–7 further increased in the LPS + rhACE2 group (*Figure 4A,4B*). As indicated by WB analysis, in mice with LPS-induced cardiac dysfunction, NLRP3 expression in heart tissue increased significantly compared with the

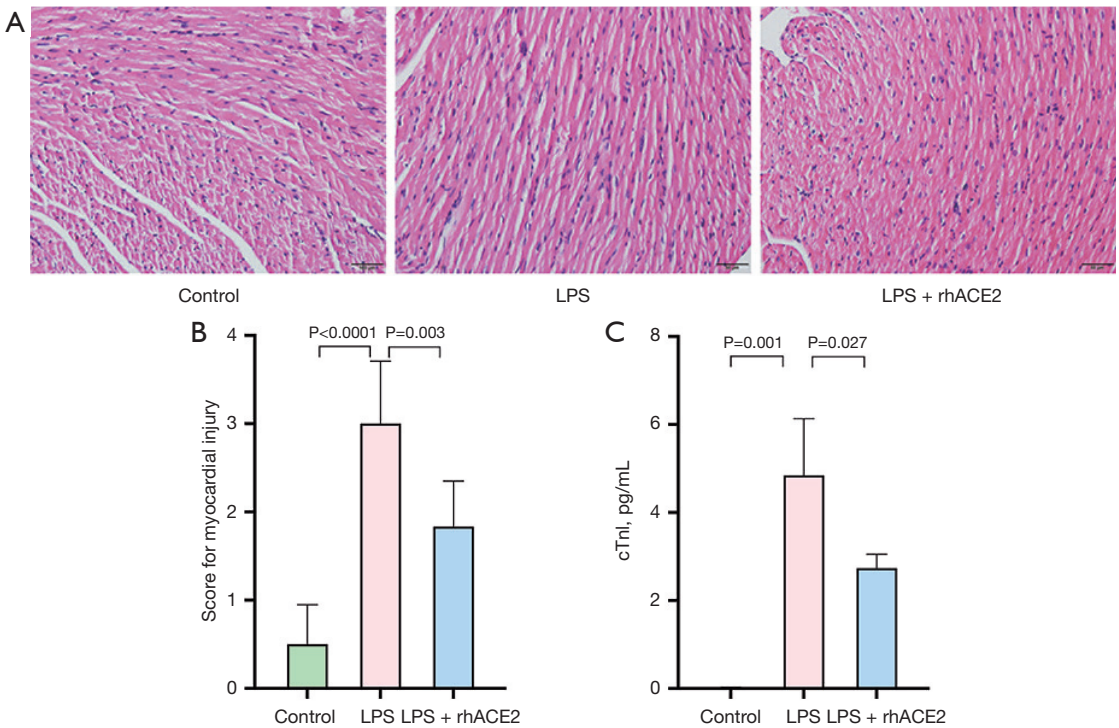


**Figure 2** RhACE2 administration relieved myocardial injury in mice with LPS-induced cardiac dysfunction. (A) Representative pictures of HE-stained heart tissue of mice in three groups (n=6). Magnification, ×200. (B) Myocardial injury score in three groups (n=6). (C) Evaluation of myocardial injury by cTnI in serum from mice in three groups (n=6). Data are expressed as mean ± SD. LPS, lipopolysaccharide; rhACE2, recombinant human angiotensin-converting enzyme 2; HE, hematoxylin and eosin, cTnI, cardiac troponin I; SD, standard deviation.

control group, but decreased significantly after rhACE2 treatment (*Figure 3A*,*3B*). The levels of Ang II in serum had a significantly positive correlation with levels of NLRP3 expression in heart tissue (*Figure 4C*).

### *RhACE2 regulated activation of the NF-κB, p38 MAPK, and AMPK pathways in heart tissue*

In order to determine the possible mechanisms and relationship between LPS-induced cardiac dysfunction and rhACE2, we further evaluated the activation levels of the NF-κB, p38 MAPK, and AMPK-α1 signaling pathways-associated proteins in heart tissue, which were involved in cardiac injury due to either Ang II/Ang 1–7 imbalance or sepsis, by WB analysis. We found that the increases of levels of p65 (a subunit of NF-κB) and p38 MAPK phosphorylation in the LPS group were diminished by rhACE2 treatment. On the contrary, levels of AMPK-α1 signaling pathway phosphorylation decreased in the LPS group and recovered partly after rhACE2 treatment (*Figure 5A-5D*).

### *A779 administration offset the inhibitive effects of rhACE2 on NLRP3 expression and cardiac-protective effects on mice with LPS-induced cardiac dysfunction*

In the second section, 12 of the total 36 mice were excluded for absence of cardiac dysfunction. Finally, 24 mice were allocated to four groups (6 per group) as described in methods and completed all the investigations. Symptoms following LPS injection were similar with those described previously. Also, all mice among groups weighed comparably and survived at 6 hours after interventions. The LVEF and LVFS of mice with LPS-induced cardiac dysfunction that were treated with both rhACE2 and A779 were lower than those of the mice were treated with rhACE2 only. The NLRP3 expression in heart tissue of mice with LPS-induced cardiac dysfunction that were treated with both rhACE2 and A779 were higher than in those that were treated with rhACE2 only. Myocardial injury and pyroptosis cell rates in mice with LPS-induced cardiac dysfunction who were treated with both rhACE2 and A779 were also higher than that who were treated

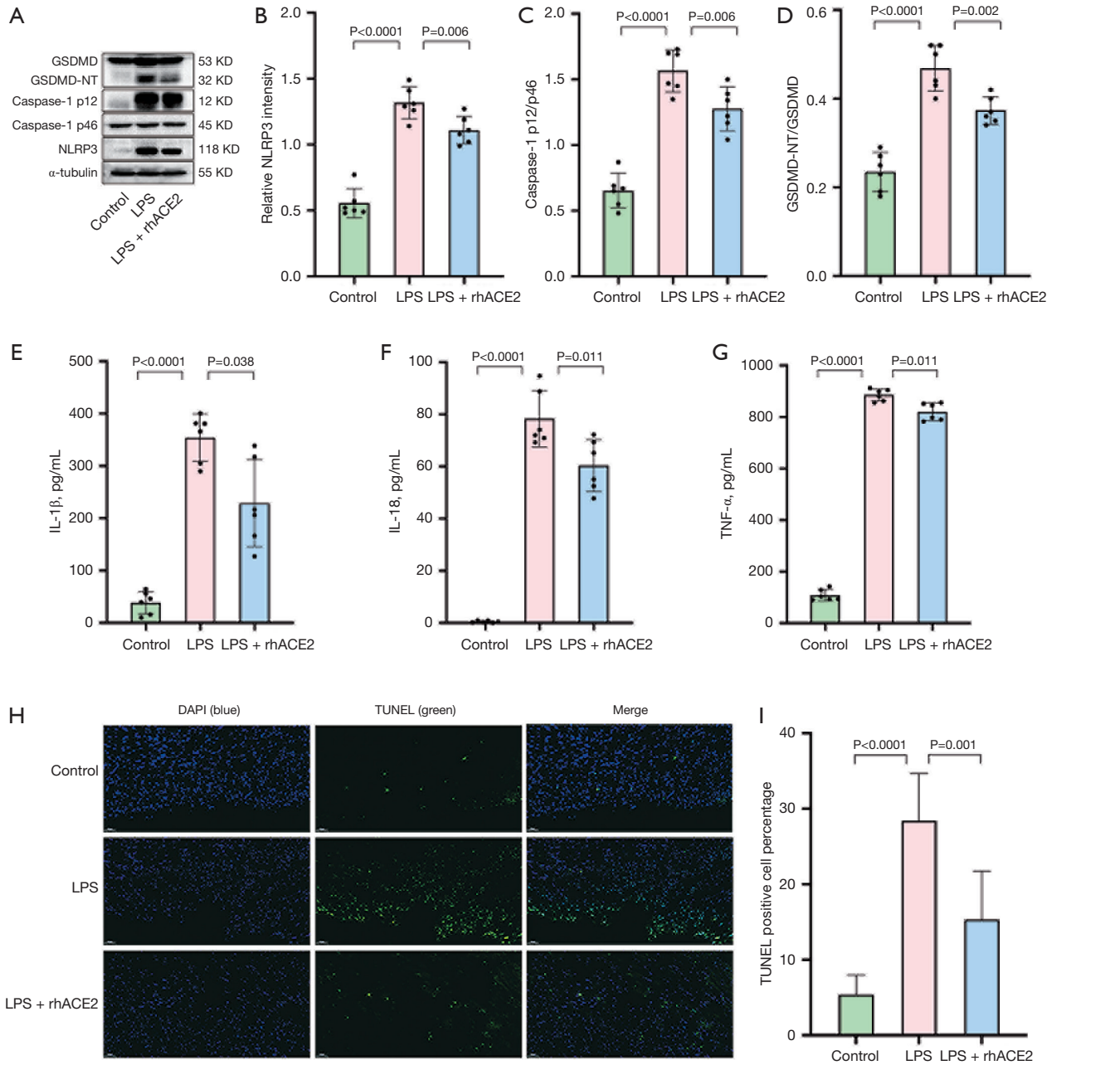


**Figure 3** RhACE2 significantly inhibited activation of NLRP3 inflammasome followed by significant decrease of NLRP3 inflammasome related inflammatory factors in serum and cell pyroptosis in heart tissues in mice with LPS-induced cardiac dysfunction. (A-D) Representative bands of WB and quantitative analysis of pyroptosis-related proteins in three groups (n=6). α-tubulin was used as an internal control. (E) The serum levels of IL-1β in three groups (n=6). (F) The serum levels of IL-18 in three groups (n=6). (G) The serum levels of TNF-α in three groups (n=6). (H) Representative images of cell pyroptosis (indicated by TUNEL positive cells) in heart tissue of mice in three groups (6 per group). Nuclei were depicted by DAPI (blue). The pyroptotic cells were depicted by TUNEL (green). Magnification, ×200. (I) Comparison of pyroptosis cell rates in heart tissue from mice in three groups (6 per group). Data are expressed as mean ± SD. GSDMD, gasdermin D; GSDMD-NT, N-terminal cleavage product of GSDMD; NLRP3, nucleotide binding and oligomerization domain-like receptor family pyrin domain-containing 3; LPS, lipopolysaccharide; rhACE2, recombinant human angiotensin-converting enzyme 2; IL, interleukin; TNF-α, tumor necrosis factor-α; DAPI, 4',6-diamidino-2-phenylindole; TUNEL, terminal deoxynucleotidyl transferase dUTP nick-end labeling; WB, western blot; SD, standard deviation.

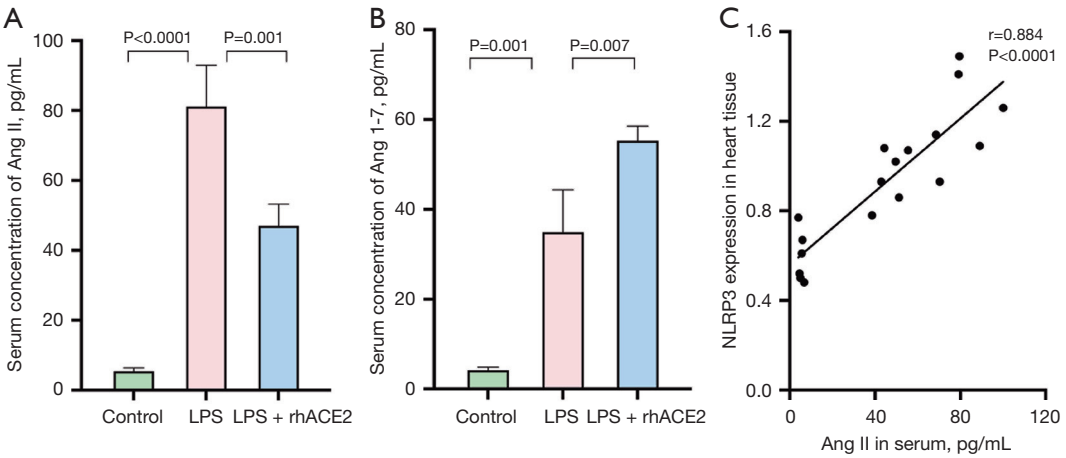


**Figure 4** RhACE2 regulated the changes of angiotensin in mice with LPS-induced cardiac dysfunction, and the levels of Ang II in serum correlated with the levels of NLRP3 expression in heart tissue positively. (A) Ang II levels in serum of mice in three groups (n=6). (B) Ang 1–7 serum levels in serum of mice in three groups (n=6). (C) Ang II levels in serum were positive correlated with levels of NLRP3 expression in heart tissue. Data are expressed as mean ± SD. Ang II, angiotensin II; LPS, lipopolysaccharide; rhACE2, recombinant human angiotensin-converting enzyme 2; Ang 1–7, angiotensin 1–7; NLRP3, nucleotide binding and oligomerization domain-like receptor family pyrin domain-containing 3; SD, standard deviation.

with rhACE2 only. Therefore, A779 administration offset the inhibitive effects of rhACE2 on NLRP3 expression and cardiac-protective effects on LPS-induced cardiac dysfunction (*Figure 6A-6F*).

## Discussion

Recently, SICD has been attracting much attention because of its contribution to mortality and complexity of management in patients with sepsis (37). However, the mechanism and treatment of SICD are still full of uncertainties. Since the hypothesis that SICM develop at the cause of gross coronary hypoperfusion was denied by the landmark study which showed the increased coronary blood flow in patients with septic shock (38), increasing numbers of studies showed disturbance of microcirculatory and microvascular thrombosis in septic heart (39,40). The notion that myocardial inhibitors, such as TNF-α, IL-1β, IL-6, ROS, and RNS (41-45), derived form either inflammation or mitochondrial dysfunction, or the crosstalk between them suppress the cardiac function is consistent with the findings that the systolic dysfunction is global (46). Additionally, influence of $Ca^{2+}$ dysregulation and β-adrenergic alteration on myocardial contractility were also discussed in detail (47-49). Disturbance of energy metabolism due to either mitochondrial dysfunction or substrate utilization disorder is hot topic in researches (50,51). Though cell death is not the significant character in septic heart, different forms of programmed myocardial cell death including apoptosis, pyroptosis, and ferroptosis have been being investigated because of their influence on inflammation and mitochondrial function (52-56). The RAAS has been a focus of research for the complex crosstalk among the components and the robust association with heart disease (19,57,58). How it is involved in sepsis had been investigated for decades (59) and attracted more attention again because of the global pandemic of COVID-19 recently for that ACE2 is known to be the receptor of SARS-CoV-2 (18). Besides the drug aimed to increase myocardial contractility and mechanical device aimed to support the cardiac pump function, various treatments targeted to regulate inflammation, mitochondrial dynamics and function, energy metabolism to improve cardiac conditions have been investigated in animal or cell experiments based on the mechanisms (60-62). However, the conclusions are variable and the data of clinical study is absence.

In this study, we demonstrated that rhACE2 regulated Ang II and Ang 1–7 serum levels followed by relief of myocardial injury and improvement of LVEF in a mouse model of LPS-induced cardiac dysfunction. The effects of rhACE2 on activations of the NF-κB, p38 MAPK, and AMPK-α1 signaling pathways that were demonstrated in the present study indicated that rhACE2 ameliorated

 

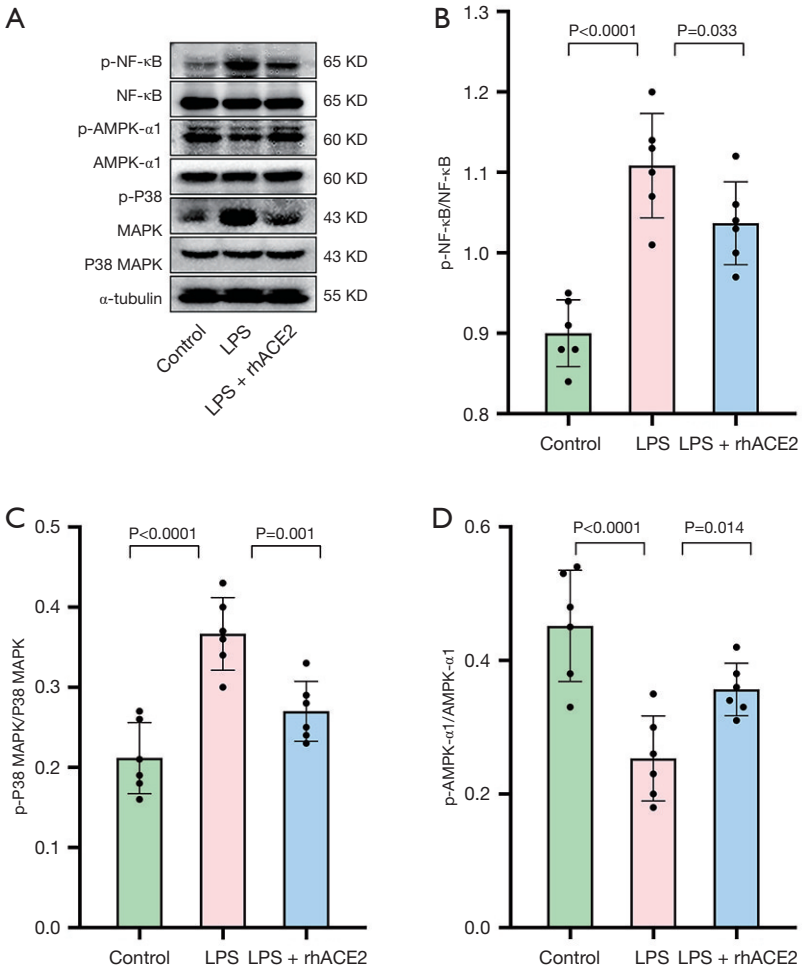


**Figure 5** RhACE2 significantly inhibited phosphorylation of NF-κB, p38 MAPK signaling pathway, and partly recovered activation of AMPK signaling pathway changed in mice with LPS-induced cardiac dysfunction. (A) Representative bands of WB and quantitative analysis of NF-κB, p38 MAPK, and AMPK-α1 signaling pathway related proteins expression in three groups. (B) Quantitative analysis phosphorylation levels of phosphorylation levels of NF-κB in three groups (n=6). (C) Quantitative analysis phosphorylation levels of p38 MAPK in three groups (n=6). (D) Quantitative analysis phosphorylation levels of AMPK-α1 in three groups (n=6). α-tubulin was used as an internal control. Data are expressed as mean ± SD. p-, phosphorylated-; NF-κB, nuclear factor κB; AMPK, AMP-activated protein kinase; MAPK, mitogen-activated protein kinase; LPS, lipopolysaccharide; rhACE2, recombinant human angiotensin-converting enzyme 2; WB, western blot; SD, standard deviation.

cardiac injury and dysfunction in mice with LPS-induced cardiac dysfunction through the NF-κB, p38 MAPK, and AMPK-α/NLRP3 inflammasome pathways depending on conversion of Ang II to Ang 1–7 during sepsis. To the best of our knowledge, the present study is the first to report the protective role of rhACE2 in SICD, in spite of a large body of research demonstrating the protective effects of rhACE2 on heart function in conditions with pressure overload, diabetic cardiomyopathy, myocardial infarction, or doxorubicin-induced cardiomyopathy.

LPS, which is a cell wall component of Gram-negative bacteria, is known to be effective to trigger an intense inflammatory response and induce sepsis (63). LPS intraperitoneal injection has been used to build an SICD model successfully for years (30,31). In the present study, LVEF declined significantly at 3 hours and reached to the bottom at 6 hours after LPS injection in about 60% of LPS treated mice, which was consistent with the data reported by a previous study (64). Changes of cTnI in serum and what were observed in HE staining heart tissue sections

showed obvious cardiac injury in mice with LPS-induced cardiac dysfunction. Using the mouse model of SICD, we elucidated the actions of rhACE2 on SICD successfully.

Various mechanisms participate in myocardial dysfunction induced by sepsis. Pyroptosis, a form of inflammation programmed cell death, is involved in either inflammatory or non-inflammatory heart disease (65,66). NLRP3 inflammasome activation plays a significant role in initiating inflammatory response and pyroptosis, contributing to cardiac injury and dysfunction in both ischemic and inflammatory heart disease (67,68).

In the present study, we observed that NLRP3 expression, caspase-1 and GSDMD activation in heart tissue increased significantly in mice with LPS-induced cardiac dysfunction, and dropped significantly under rhACE2 treatment. Up-regulation of pyroptotic cell rates in heart tissue indicated by TUNEL staining, and increase of IL-1β and IL-18 in serum of mice with SICD were also diminished by rhACE2 treatment in our study. According to previous report, increase of NLRP3 protein expression is the priming step of NLRP3 inflammasome activation (27). Caspase-1, the key effector of NLRP3 inflammasome, self-cleaves to active caspase-1 on the platform NLRP3 assembled during activation. Active caspase-1 then promotes pro-IL-1β and pro-IL-18 maturate to IL-1β and IL-18 and cleaves GSDMD to free its N-terminal domain and induce the formation of pores at the membrane, leading to pyroptosis (69). TNF-α is a main inflammatory cytokine in sepsis. Maturation and release of IL-1β and IL-18 amplify the inflammatory response as indicated by the changes of TNF-α among groups in the study. TNF-α and IL-1β are regarded as the main myocardial inhibitors in septic shock contribute to cardiac depression. Pyroptosis procedure mediated by GSDMD cleavage has a detrimental effect on cardiac function (70). Inhibitors of NLRP3 inflammasome-related pro-inflammatory factors and depletion of pyroptosis by knocking out NLRP3 or other components of NLRP3 inflammasome (ASC, GSDMD, or caspase-1) attenuate cardiac injury and improve cardiac function (67,68,70-72). Our observation in the present study also indicated the involvement of NLRP3 inflammasome activation in LPS-induced cardiac dysfunction. Further, the inhibitive role of rhACE2 on NLRP3 inflammasome activation as well as the following inflammatory response and cell pyroptosis demonstrated in our study is the probable mechanism of the protective role of rhACE2 in SICD. This is also consistent with previous researches reporting that rhACE2 shows a protective role in sepsis-induced organ injury (26,33), and cardiac dysfunction caused by doxorubicin (73) through inhibition of NLRP3 inflammasome.

As a negative regulator of RAAS, ACE2 catalyzes the vasoconstrictive, pro-inflammatory, and fibrogenic Ang II peptide to the vasodilatory, anti-inflammatory, and anti-fibrogenic Ang 1–7 peptide, which plays a protective role in heart disease (74,75). The catalyzing action from Ang II to Ang 1–7 of rhACE2 was also revealed in our study. Ang II in serum increased significantly in the LPS group, and dropped significantly in the LPS + rhACE2 group. In contrast, Ang 1–7 concentrations went up significantly in the LPS group and further increased in the LPS + rhACE2 group. Increase of Ang II and Ang 1–7 in LPS group just the results of activation of RAAS during sepsis and SICD. Decrease of Ang II and Increase of Ang 1–7 indicated the converting action of rhACE2 on Ang II. Additionally, our

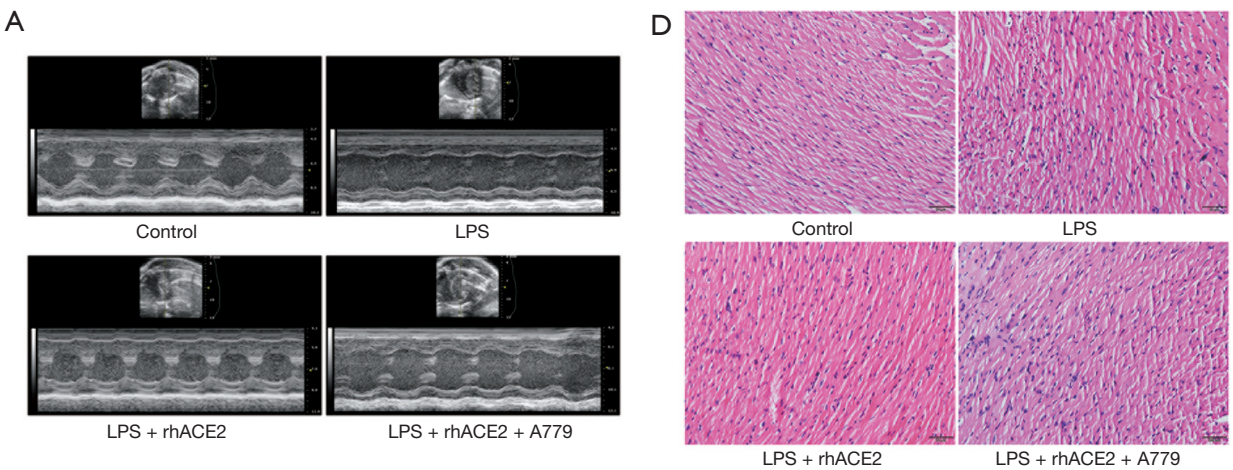

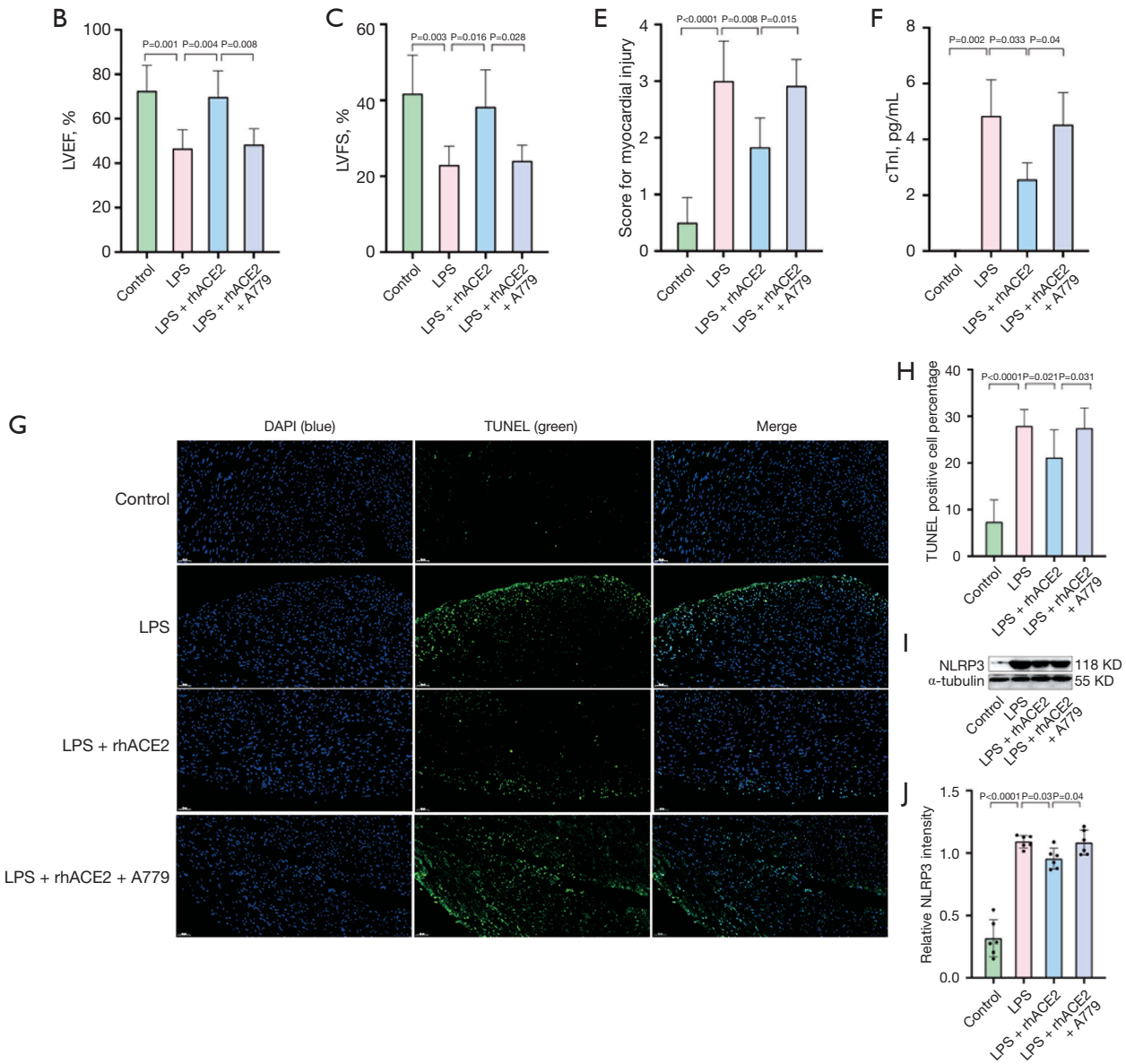


**Figure 6** A779 administration offset the improve effect of rhACE2 in mice with LPS-induced cardiac dysfunction. (A) Transthoracic echocardiography (M-mode) of mice in each group (6 per group). (B) Comparison of LVEF of mice among four groups (6 per group). (C) Comparison of LVFS of mice among four groups (6 per group). (D) Representative pictures of HE-stained heart tissue of mice in four groups (n=6). Magnification, ×200. (E) Myocardial injury score in four groups (n=6). (F) Evaluation of myocardial injury by cTnI in serum from mice in four groups (n=6). (G) Representative images of cell pyroptosis (indicated by TUNEL labeled cells) in heart tissue of mice in four groups (6 per group). Nuclei were depicted by DAPI (blue). The pyroptotic cells were depicted by TUNEL (green). Magnification, ×200. (H) Comparison of pyroptosis cell rates in heart tissue from mice in four groups (6 per group). (I) WB for NLRP3 expression in heart tissue of mice from four groups (n=6), α-tubulin was used as an internal control. (J) Quantitative analysis of NLRP3 expression in heart tissue of mice from four groups (n=6). Data are expressed as mean ± SD. LPS, lipopolysaccharide; rhACE2, recombinant human angiotensin-converting enzyme 2; LVEF, left ventricular ejection fraction; LVFS, left ventricular fractional shortening; DAPI, 4',6-diamidino-2-phenylindole; TUNEL, terminal deoxynucleotidyl transferase dUTP nick-end labeling; NLRP3, nucleotide binding and oligomerization domain-like receptor family pyrin domain-containing 3; HE, hematoxylin and eosin; cTnI, cardiac troponin I; WB, western blot; SD, standard deviation.

study showed that changes of NLRP3 expression in heart tissue were significantly positively correlated with the changes of Ang II in serum. Therefore, it could be Ang II that influenced the NLRP3 expression in heart tissue and caused cardiac injury. In fact, Ang II has been shown by previous reports to induce NLRP3 and reactive oxygen species (ROS) production which participates the disturbed redox cycle in sepsis and leads to cardiac injury and dysfunction (76,77).

Ang 1–7, the effects of which are opposite to those of Ang II, exerts its effects of inhibiting NLRP3 inflammasome activation through the Mas receptor and is implicated in physiological and pathophysiological processes, including leukocyte recruitment and inflammation, cardiac remodeling, and vascular alteration (78,79). Mice deficient for Mas receptor show cardiovascular-related phenotypes, including myocardial contractile dysfunction and endothelial dysfunction (74,80,81). On the contrary, increase of Ang 1–7 in the heart by either infusion or overexpression from transgenes elicited cardioprotective actions in cardiac damage models (82,83). When A779, a selective mas receptor antagonist of Ang 1–7, was administrated to mice with SICD, the protective role of rhACE2 on cardiac injury and function as well as the inhibitive role of it on NLRP3 expression were offset according to our study.

Not only A779 offset LVEF improve due to rhACE2 treatment in mice with SICD, but it also offset the effects of rhACE2 treatment on changes of cTnI concentration in serum, cell pyroptosis in heart tissue and myocardial injury induced by LPS insult. Furthermore, administration of A779 offset the increase of NLRP3 induced by LPS insult. What were observed in the A779 part of the experiment verified that the protective effects of rhACE2 on SICD depended on its conversion action of Ang II and the resulting increase of Ang 1–7. The results are similar to the report of Liu *et al.*, in which A779 offset the beneficial effects on acute lung injury resulted from sepsis (84).

As shown in this study, rhACE2 treatment decreased Ang II and further enhanced Ang 1-7 in serum of mice with SICD. In line with the activation of NLRP3 inflammasome, the NF-κB and p38 MAPK signaling pathways were activated in mice with LPS induced cardiac dysfunction. In line with the suppression of NLRP3 inflammasome activation by rhACE2 treatment, activation of the NF-κB and p38 MAPK signaling pathways were also suppressed in mice with LPS-induced cardiac dysfunction. Therefore, we inferred that the NF-κB and p38 MAPK signaling pathways were involved in the protective role of rhACE2 in SICD. The activation of toll-like receptors (TLRs)/NF-κB has been extensively accepted as pathways contributing to development of sepsis and following MODS including SICD (85). In response to microbial molecules, NF-κB stimulates the expression of NLRP3, which is the priming step of canonical NLRP3 inflammasome activation (69,86,87). Also, previous researches demonstrated that p38 MAPK plays a role in inflammasome priming signals (88) and regulation of downstream p38 MAPK activation is critical for NLRP3 expression and caspase-1 activation (89). It has been reported that the p38 MAPK pathway is closely related to LPS-induced septic shock (90). A recent study demonstrated that activation of the p38 MAPK pathway promotes NLRP3 inflammasome activation in septic shock (91). Ang II has been shown to induce NLRP3, in various cardiac cells in a non-septic cardiac damage model, depending on the AT1R/NF-κB or p38 MAPK pathway or crosstalk among them (76,77,92). By contrast, Ang 1–7 has inhibitory effects on activated NF-κB and p38 MAPK pathways in these cells (93) and is beneficial for improved contractility (94).

Additionally, in the present study, the AMPK-α1 signaling pathway was inhibited in mice with LPS-induced cardiac dysfunction and was partly recovered by rhACE2 administration. Previous reports have shown that AMPK activation inhibited NLRP3 inflammasome-induced pyroptosis in microglia (95) and relieved myocardial dysfunction through the AMPK-α/NLRP3 inflammasome dependent pathway (96). Deficiency of AMPK-α1 influences systemic production of cytokines and results in lung injury, liver damage after sepsis, and exacerbates sepsis-induced mortality in male mice (97). Evidence showed that ACE2 deficiency impaired cardiac function and contributed to suppressing the phosphorylation of AMPK, aggravating cardiac lipotoxicity, and myocardial insulin resistance (98). In contrast, increasing activation of AMPK-α and the PI3K/AKT pathway by an ACE2 activator improved cardiac function in diabetic cardiomyopathy (99). Therefore, enhancement of AMPK-α1 activation could represent another signaling pathway with a protective role of rhACE2 to SICD.

Thus, multiple mechanisms, including the NF-κB, p38 MAPK, and AMPK-α1 signaling pathways, were involved in the cardiac protective role of rhACE2 in SICD depending on converting Ang II to Ang 1–7 followed by the regulation of activation of NLRP3 inflammasome. By modulating NLRP3 inflammasome activation, rhACE2 is supposed to regulating the followed inflammatory process and redox

imbalance in septic heart, which might protect the heart from injury.

In summary, we established a model of SICD *in vivo* with mouse and detected the beneficial role of rhACE2 on SICD; the results might provide a new direction of management for patients with SICD.

Additionally, as the receptor of the novel SARS-CoV-2, ACE2 mediates the entry of virus into cells, contributing to the subsequent infection and pathological process such as inflammation and organ injury (18). There are two forms of ACE2 existing in plasma (which is named soluble ACE2, sACE2) and anchoring on cell membrane respectively. It is the membrane-located ACE2 that can be bound to the viral surface spike protein to facilitate the virus internalization and subsequent replication (100). Additionally, the entry of virus mediated by transmembrane ACE2 led to down-regulation of the trans-membrane ACE2 followed by increase of local Ang II which aggravated the inflammation in tissue (18). As a competitive interceptor, sACE2 can neutralize the viruses and block their entry into target cells. It is verified by the study in which soluble rhACE2 inhibited SARS-CoV-2 infection in engineered human tissues (101). Therefore, supplementing soluble rhACE2 to patients with SARS-CoV-2 infection is expected to benefit the population through both infection control and RAAS negative modulation and deserves further investigation in preclinical and clinical settings.

### *Limitations*

Compared with the CLP model, the SICD model in the present study, which was established via LPS intraperitoneal injection, does not simulate the common pattern of sepsis well in clinical conditions, since sepsis often derives from infection caused by either Gram-negative, or Gram-positive bacterial, or both of them. However, management of cardiac dysfunction induced by endotoxemia, which excludes the influence of unsatisfactory infection control on progression of sepsis and organ injury, can clarify the effects of the intervention aiming to more adequately modulate the dysregulated host response to infection.

In the absence of hemodynamic monitoring, we could not provide accuracy data on preload and could not clarify the influence of fluid resuscitation on LVEF. However, the left ventricular end diastolic volume (LVEDV) of mice among groups were comparable (Figure S1), which indicated the comparable preload among groups in a certain degree.

In the absence of a cell experiment, we could not present the cell-specific effects of rhACE2 on SICD, especially effects on cardiomyocytes. Indeed, in our study, the main pathologic discovery of heart section was not cardiomyocyte necrosis but infiltration, interstitial edema, and cardiomyocyte disorders. Consistently, cardiomyocyte necrosis is probably of less importance as it has been found only in a small proportion of human autopsy specimens, and its occurrence during experimental sepsis has not been universally confirmed (102). In fact, pyroptosis occurred not only in cradiomyocytes, but also in immune cells, cardiac fibroblast cells, and endothelial cells that exist in heart tissue and amplified inflammatory, which contributes to the reversible functional damage of the septic heart (30,103-106).

Only function of the left heart was evaluated in our study. Since it is common (107) and associates with higher short-term and long-term mortality during sepsis (108), right ventricular (RV) function in sepsis is worthy of further investigation to compensate our understanding of SICD, which will be taken into consideration in our subsequent studies.

Additionally, cardiac diastolic dysfunction was also detected in patients with SICD (9). However, we did not detect a significant difference among groups when we examined the diastolic function of left ventricle by E/A (Figure S2). A better animal model is needed to evaluate the diastolic function of the septic heart and further study is needed to explore the management of diastolic dysfunction of SICD.

## Conclusions

In conclusion, rhACE2 played a protective role in the SICD mice model, ameliorating cardiac injury and contractile dysfunction in mice with LPS-induced cardiac dysfunction through the NF-κB, p38 MAPK, and AMPK-α1/NLRP3 inflammasome pathway dependent on converting Ang II to Ang 1–7. These findings provide a new idea about research and management of SICD.

Well-designed preclinical and clinical studies are needed to investigate the exact influence and mechanism of rhACE2 on SICD in depth, which are expected to enable a precise understanding and treatment of SICD.

## Acknowledgments

*Funding:* This study was supported by the Department of Science and Technology of Hebei Province of China (No. 20277707D).

 

## Footnote

*Reporting Checklist:* The authors have completed the ARRIVE reporting checklist. Available at https://atm.amegroups.com/article/view/10.21037/atm-22-6016/rc

*Data Sharing Statement:* Available at https://atm.amegroups.com/article/view/10.21037/atm-22-6016/dss

*Conflicts of Interest:* All authors have completed the ICMJE uniform disclosure form (available at https://atm.amegroups.com/article/view/10.21037/atm-22-6016/coif). The authors have no conflicts of interest to declare.

*Ethical Statement:* The authors are accountable for all aspects of the work in ensuring that questions related to the accuracy or integrity of any part of the work are appropriately investigated and resolved. Animal experiments were performed under a project license (No. 2020002) granted by the laboratory animal ethical committee of Animal Experiment Center of the Fourth Hospital of Hebei Medical University, complying with the Guide for the Care and Use of Laboratory Animals of Institutes of Health (Eighth Edition). Hebei Key Laboratory of Critical Disease Mechanism and Intervention was informed and agreed with this study.



## References

1. Singer M, Deutschman CS, Seymour CW, et al. The Third International Consensus Definitions for Sepsis and Septic Shock (Sepsis-3). JAMA 2016;315:801-10.
2. Xie J, Wang H, Kang Y, et al. The Epidemiology of Sepsis in Chinese ICUs: A National Cross-Sectional Survey. Crit Care Med 2020;48:e209-18.
3. Imaeda T, Nakada TA, Takahashi N, et al. Trends in the incidence and outcome of sepsis using data from a Japanese nationwide medical claims database-the Japan Sepsis Alliance (JaSA) study group. Crit Care 2021;25:338.
4. Vincent JL, Jones G, David S, et al. Frequency and mortality of septic shock in Europe and North America: a systematic review and meta-analysis. Crit Care 2019;23:196.
5. Markwart R, Saito H, Harder T, et al. Epidemiology and burden of sepsis acquired in hospitals and intensive care units: a systematic review and meta-analysis. Intensive Care Med 2020;46:1536-51.
6. Kahn JM, Davis BS, Yabes JG, et al. Association Between State-Mandated Protocolized Sepsis Care and In-hospital Mortality Among Adults With Sepsis. JAMA 2019;322:240-50.
7. Bauer M, Gerlach H, Vogelmann T, et al. Mortality in sepsis and septic shock in Europe, North America and Australia between 2009 and 2019- results from a systematic review and meta-analysis. Crit Care 2020;24:239.
8. Hollenberg SM, Singer M. Pathophysiology of sepsis-induced cardiomyopathy. Nat Rev Cardiol 2021;18:424-34.
9. Ehrman RR, Sullivan AN, Favot MJ, et al. Pathophysiology, echocardiographic evaluation, biomarker findings, and prognostic implications of septic cardiomyopathy: a review of the literature. Crit Care 2018;22:112.
10. Parrillo JE, Parker MM, Natanson C, et al. Septic shock in humans. Advances in the understanding of pathogenesis, cardiovascular dysfunction, and therapy. Ann Intern Med 1990;113:227-42.
11. Bitker L, Burrell LM. Classic and Nonclassic Renin-Angiotensin Systems in the Critically Ill. Crit Care Clin 2019;35:213-27.
12. Gallagher PE, Ferrario CM, Tallant EA. Regulation of ACE2 in cardiac myocytes and fibroblasts. Am J Physiol Heart Circ Physiol 2008;295:H2373-9.
13. Schäfer A, Fraccarollo D, Tas P, et al. Endothelial dysfunction in congestive heart failure: ACE inhibition vs. angiotensin II antagonism. Eur J Heart Fail 2004;6:151-9.
14. Crowley SD, Rudemiller NP. Immunologic Effects of the Renin-Angiotensin System. J Am Soc Nephrol 2017;28:1350-61.
15. Mascolo A, Scavone C, Rafaniello C, et al. Renin-Angiotensin System and Coronavirus Disease 2019: A Narrative Review. Front Cardiovasc Med 2020;7:143.
16. Rossi F, Mascolo A, Mollace V. The pathophysiological role of natriuretic peptide-RAAS cross talk in heart failure. Int J Cardiol 2017;226:121-5.
17. Santos RA, Ferreira AJ, Verano-Braga T, et al. Angiotensin-converting enzyme 2, angiotensin-(1-7)

 

and Mas: new players of the renin-angiotensin system. J Endocrinol 2013;216:R1-R17.
18. Gheblawi M, Wang K, Viveiros A, et al. Angiotensin-Converting Enzyme 2: SARS-CoV-2 Receptor and Regulator of the Renin-Angiotensin System: Celebrating the 20th Anniversary of the Discovery of ACE2. Circ Res 2020;126:1456-74.
19. Zhong J, Basu R, Guo D, et al. Angiotensin-converting enzyme 2 suppresses pathological hypertrophy, myocardial fibrosis, and cardiac dysfunction. Circulation 2010;122:717-28, 18 p following 728.
20. Patel VB, Zhong JC, Grant MB, et al. Role of the ACE2/Angiotensin 1-7 Axis of the Renin-Angiotensin System in Heart Failure. Circ Res 2016;118:1313-26.
21. Yamaguchi N, Jesmin S, Zaedi S, et al. Time-dependent expression of renal vaso-regulatory molecules in LPS-induced endotoxemia in rat. Peptides 2006;27:2258-70.
22. Gupta A, Rhodes GJ, Berg DT, et al. Activated protein C ameliorates LPS-induced acute kidney injury and downregulates renal INOS and angiotensin 2. Am J Physiol Renal Physiol 2007;293:F245-54.
23. Ji Y, Ren X, Zhao Y, et al. Role of intracardiac angiotensin II in cardiac dysfunction of rat during septic shock. Chin Med J (Engl) 1996;109:864-7.
24. Hirano Y, Takeuchi H, Suda K, et al. (Pro)renin receptor blocker improves survival of rats with sepsis. J Surg Res 2014;186:269-77.
25. Haschke M, Schuster M, Poglitsch M, et al. Pharmacokinetics and pharmacodynamics of recombinant human angiotensin-converting enzyme 2 in healthy human subjects. Clin Pharmacokinet 2013;52:783-92.
26. Khan A, Benthin C, Zeno B, et al. A pilot clinical trial of recombinant human angiotensin-converting enzyme 2 in acute respiratory distress syndrome. Crit Care 2017;21:234.
27. Pellegrini C, Antonioli L, Lopez-Castejon G, et al. Canonical and Non-Canonical Activation of NLRP3 Inflammasome at the Crossroad between Immune Tolerance and Intestinal Inflammation. Front Immunol 2017;8:36.
28. Busch K, Kny M, Huang N, et al. Inhibition of the NLRP3/IL-1β axis protects against sepsis-induced cardiomyopathy. J Cachexia Sarcopenia Muscle 2021;12:1653-68.
29. Sun NN, Yu CH, Pan MX, et al. Mir-21 Mediates the Inhibitory Effect of Ang (1-7) on AngII-induced NLRP3 Inflammasome Activation by Targeting Spry1 in lung fibroblasts. Sci Rep 2017;7:14369.
30. Li N, Zhou H, Wu H, et al. STING-IRF3 contributes to lipopolysaccharide-induced cardiac dysfunction, inflammation, apoptosis and pyroptosis by activating NLRP3. Redox Biol 2019;24:101215.
31. Zhang Y, Buzukela A, Peng P. Advances in animal models of sepsis-induced myocardial dysfunction. Zhonghua Wei Zhong Bing Ji Jiu Yi Xue 2019;31:785-8.
32. Shi J, Chen Y, Zhi H, et al. Levosimendan protects from sepsis-inducing cardiac dysfunction by suppressing inflammation, oxidative stress and regulating cardiac mitophagy via the PINK-1-Parkin pathway in mice. Ann Transl Med 2022;10:212.
33. Imai Y, Kuba K, Rao S, et al. Angiotensin-converting enzyme 2 protects from severe acute lung failure. Nature 2005;436:112-6.
34. Chen QF, Kuang XD, Yuan QF, et al. Lipoxin A(4) attenuates LPS-induced acute lung injury via activation of the ACE2-Ang-(1-7)-Mas axis. Innate Immun 2018;24:285-96.
35. Xu S, Wu B, Zhong B, et al. Naringenin alleviates myocardial ischemia/reperfusion injury by regulating the nuclear factor-erythroid factor 2-related factor 2 (Nrf2)/System xc-/glutathione peroxidase 4 (GPX4) axis to inhibit ferroptosis. Bioengineered 2021;12:10924-34.
36. Sen Z, Jie M, Jingzhi Y, et al. Total Coumarins from Hydrangea paniculata Protect against Cisplatin-Induced Acute Kidney Damage in Mice by Suppressing Renal Inflammation and Apoptosis. Evid Based Complement Alternat Med 2017;2017:5350161.
37. Pulido JN, Afessa B, Masaki M, et al. Clinical spectrum, frequency, and significance of myocardial dysfunction in severe sepsis and septic shock. Mayo Clin Proc 2012;87:620-8.
38. Dhainaut JF, Huyghebaert MF, Monsallier JF, et al. Coronary hemodynamics and myocardial metabolism of lactate, free fatty acids, glucose, and ketones in patients with septic shock. Circulation 1987;75:533-41.
39. Doerschug KC, Delsing AS, Schmidt GA, et al. Renin-angiotensin system activation correlates with microvascular dysfunction in a prospective cohort study of clinical sepsis. Crit Care 2010;14:R24.
40. Senatore F, Balakumar P, Jagadeesh G. Dysregulation of the renin-angiotensin system in septic shock: Mechanistic insights and application of angiotensin II in clinical management. Pharmacol Res 2021;174:105916.
41. Kumar A, Thota V, Dee L, et al. Tumor necrosis factor alpha and interleukin 1beta are responsible for in vitro myocardial cell depression induced by human septic shock

 

serum. J Exp Med 1996;183:949-58.
42. Haileselassie B, Su E, Pozios I, et al. Myocardial oxidative stress correlates with left ventricular dysfunction on strain echocardiography in a rodent model of sepsis. Intensive Care Med Exp 2017;5:21.
43. Ferdinandy P, Danial H, Ambrus I, et al. Peroxynitrite is a major contributor to cytokine-induced myocardial contractile failure. Circ Res 2000;87:241-7.
44. Kumar A, Brar R, Wang P, et al. Role of nitric oxide and cGMP in human septic serum-induced depression of cardiac myocyte contractility. Am J Physiol 1999;276:R265-76.
45. Monteiro VVS, Reis JF, de Souza Gomes R, et al. Dual Behavior of Exosomes in Septic Cardiomyopathy. Adv Exp Med Biol 2017;998:101-12.
46. Zanotti-Cavazzoni SL, Hollenberg SM. Cardiac dysfunction in severe sepsis and septic shock. Curr Opin Crit Care 2009;15:392-7.
47. Layland J, Cave AC, Warren C, et al. Protection against endotoxemia-induced contractile dysfunction in mice with cardiac-specific expression of slow skeletal troponin I. FASEB J 2005;19:1137-9.
48. Hobai IA, Edgecomb J, LaBarge K, et al. Dysregulation of intracellular calcium transporters in animal models of sepsis-induced cardiomyopathy. Shock 2015;43:3-15.
49. Rudiger A. Beta-block the septic heart. Crit Care Med 2010;38:S608-12.
50. Preau S, Vodovar D, Jung B, et al. Energetic dysfunction in sepsis: a narrative review. Ann Intensive Care 2021;11:104.
51. Wasyluk W, Nowicka-Stążka P, Zwolak A. Heart Metabolism in Sepsis-Induced Cardiomyopathy-Unusual Metabolic Dysfunction of the Heart. Int J Environ Res Public Health 2021;18:7598.
52. Beranek JT. Cardiomyocyte apoptosis contributes to the pathology of the septic shock heart. Intensive Care Med 2002;28:218; author reply 219.
53. Tu GW, Ma JF, Li JK, et al. Exosome-Derived From Sepsis Patients' Blood Promoted Pyroptosis of Cardiomyocytes by Regulating miR-885-5p/HMBOX1. Front Cardiovasc Med 2022;9:774193.
54. Teng Y, Li N, Wang Y, et al. NRF2 Inhibits Cardiomyocyte Pyroptosis Via Regulating CTRP1 in Sepsis-Induced Myocardial Injury. Shock 2022;57:590-9.
55. Zheng X, Chen W, Gong F, et al. The Role and Mechanism of Pyroptosis and Potential Therapeutic Targets in Sepsis: A Review. Front Immunol 2021;12:711939.
56. Li N, Wang W, Zhou H, et al. Ferritinophagy-mediated ferroptosis is involved in sepsis-induced cardiac injury. Free Radic Biol Med 2020;160:303-18.
57. Verano-Braga T, Martins ALV, Motta-Santos D, et al. ACE2 in the renin-angiotensin system. Clin Sci (Lond) 2020;134:3063-78.
58. Oudit GY, Crackower MA, Backx PH, et al. The role of ACE2 in cardiovascular physiology. Trends Cardiovasc Med 2003;13:93-101.
59. Ning L, Rong J, Zhang Z, et al. Therapeutic approaches targeting renin-angiotensin system in sepsis and its complications. Pharmacol Res 2021;167:105409.
60. Ravikumar N, Sayed MA, Poonsuph CJ, et al. Septic Cardiomyopathy: From Basics to Management Choices. Curr Probl Cardiol 2021;46:100767.
61. L'Heureux M, Sternberg M, Brath L, et al. Sepsis-Induced Cardiomyopathy: a Comprehensive Review. Curr Cardiol Rep 2020;22:35.
62. Mokhtari B, Yavari R, Badalzadeh R, et al. An Overview on Mitochondrial-Based Therapies in Sepsis-Related Myocardial Dysfunction: Mitochondrial Transplantation as a Promising Approach. Can J Infect Dis Med Microbiol 2022;2022:3277274.
63. De Castro C, Holst O, Lanzetta R, et al. Bacterial lipopolysaccharides in plant and mammalian innate immunity. Protein Pept Lett 2012;19:1040-4.
64. Wang H, Bei Y, Shen S, et al. miR-21-3p controls sepsis-associated cardiac dysfunction via regulating SORBS2. J Mol Cell Cardiol 2016;94:43-53.
65. Liu JJ, Li Y, Yang MS, et al. SP1-induced ZFAS1 aggravates sepsis-induced cardiac dysfunction via miR-590-3p/NLRP3-mediated autophagy and pyroptosis. Arch Biochem Biophys 2020;695:108611.
66. Del Re DP, Amgalan D, Linkermann A, et al. Fundamental Mechanisms of Regulated Cell Death and Implications for Heart Disease. Physiol Rev 2019;99:1765-817.
67. Zhang J, Huang L, Shi X, et al. Metformin protects against myocardial ischemia-reperfusion injury and cell pyroptosis via AMPK/NLRP3 inflammasome pathway. Aging (Albany NY) 2020;12:24270-87.
68. Pappritz K, Lin J, El-Shafeey M, et al. Colchicine prevents disease progression in viral myocarditis via modulating the NLRP3 inflammasome in the cardiosplenic axis. ESC Heart Fail 2022;9:925-41.
69. Paik S, Kim JK, Silwal P, et al. An update on the regulatory mechanisms of NLRP3 inflammasome activation. Cell Mol Immunol 2021;18:1141-60.
70. Zeng C, Duan F, Hu J, et al. NLRP3 inflammasome-mediated pyroptosis contributes to the pathogenesis

 

of non-ischemic dilated cardiomyopathy. Redox Biol 2020;34:101523.
71. Toldo S, Marchetti C, Mauro AG, et al. Inhibition of the NLRP3 inflammasome limits the inflammatory injury following myocardial ischemia-reperfusion in the mouse. Int J Cardiol 2016;209:215-20.
72. Hillestad V, Espe EK, Cero F, et al. IL-18 neutralization during alveolar hypoxia improves left ventricular diastolic function in mice. Acta Physiol (Oxf) 2015;213:492-504.
73. Ma H, Kong J, Wang YL, et al. Angiotensin-converting enzyme 2 overexpression protects against doxorubicin-induced cardiomyopathy by multiple mechanisms in rats. Oncotarget 2017;8:24548-63.
74. Crackower MA, Sarao R, Oudit GY, et al. Angiotensin-converting enzyme 2 is an essential regulator of heart function. Nature 2002;417:822-8.
75. Fosbøl EL, Butt JH, Østergaard L, et al. Association of Angiotensin-Converting Enzyme Inhibitor or Angiotensin Receptor Blocker Use With COVID-19 Diagnosis and Mortality. JAMA 2020;324:168-77.
76. Lim S, Lee ME, Jeong J, et al. sRAGE attenuates angiotensin II-induced cardiomyocyte hypertrophy by inhibiting RAGE-NFκB-NLRP3 activation. Inflamm Res 2018;67:691-701.
77. Lv SL, Zeng ZF, Gan WQ, et al. Lp-PLA2 inhibition prevents Ang II-induced cardiac inflammation and fibrosis by blocking macrophage NLRP3 inflammasome activation. Acta Pharmacol Sin 2021;42:2016-32.
78. Simões e Silva AC, Silveira KD, Ferreira AJ, et al. ACE2, angiotensin-(1-7) and Mas receptor axis in inflammation and fibrosis. Br J Pharmacol 2013;169:477-92.
79. You Y, Huang Y, Wang D, et al. Angiotensin (1-7) inhibits arecoline-induced migration and collagen synthesis in human oral myofibroblasts via inhibiting NLRP3 inflammasome activation. J Cell Physiol 2019;234:4668-80.
80. Santos RA, Castro CH, Gava E, et al. Impairment of in vitro and in vivo heart function in angiotensin-(1-7) receptor MAS knockout mice. Hypertension 2006;47:996-1002.
81. Rabelo LA, Xu P, Todiras M, et al. Ablation of angiotensin (1-7) receptor Mas in C57Bl/6 mice causes endothelial dysfunction. J Am Soc Hypertens 2008;2:418-24.
82. Der Sarkissian S, Grobe JL, Yuan L, et al. Cardiac overexpression of angiotensin converting enzyme 2 protects the heart from ischemia-induced pathophysiology. Hypertension 2008;51:712-8.
83. Santos RA, Ferreira AJ, Nadu AP, et al. Expression of an angiotensin-(1-7)-producing fusion protein produces cardioprotective effects in rats. Physiol Genomics 2004;17:292-9.
84. Liu J, Chen Q, Liu S, et al. Sini decoction alleviates E. coli induced acute lung injury in mice via equilibrating ACE-AngII-AT1R and ACE2-Ang-(1-7)-Mas axis. Life Sci 2018;208:139-48. Erratum in: Life Sci 2019;239:116983.
85. Wang R, Xu Y, Fang Y, et al. Pathogenetic mechanisms of septic cardiomyopathy. J Cell Physiol 2022;237:49-58.
86. Bauernfeind FG, Horvath G, Stutz A, et al. Cutting edge: NF-kappaB activating pattern recognition and cytokine receptors license NLRP3 inflammasome activation by regulating NLRP3 expression. J Immunol 2009;183:787-91.
87. Han Y, Sun HJ, Tong Y, et al. Curcumin attenuates migration of vascular smooth muscle cells via inhibiting NFκB-mediated NLRP3 expression in spontaneously hypertensive rats. J Nutr Biochem 2019;72:108212.
88. Wang C, Hockerman S, Jacobsen EJ, et al. Selective inhibition of the p38alpha MAPK-MK2 axis inhibits inflammatory cues including inflammasome priming signals. J Exp Med 2018;215:1315-25.
89. Moon JS, Lee S, Park MA, et al. UCP2-induced fatty acid synthase promotes NLRP3 inflammasome activation during sepsis. J Clin Invest 2015;125:78253.
90. Nold MF, Nold-Petry CA, Fischer D, et al. Activated protein C downregulates p38 mitogen-activated protein kinase and improves clinical parameters in an in-vivo model of septic shock. Thromb Haemost 2007;98:1118-26.
91. Dong R, Xue Z, Fan G, et al. Pin1 Promotes NLRP3 Inflammasome Activation by Phosphorylation of p38 MAPK Pathway in Septic Shock. Front Immunol 2021;12:620238.
92. Takata Y, Liu J, Yin F, et al. PPARdelta-mediated antiinflammatory mechanisms inhibit angiotensin II-accelerated atherosclerosis. Proc Natl Acad Sci U S A 2008;105:4277-82.
93. Su Z, Zimpelmann J, Burns KD. Angiotensin-(1-7) inhibits angiotensin II-stimulated phosphorylation of MAP kinases in proximal tubular cells. Kidney Int 2006;69:2212-8.
94. Zhu S, Xu T, Luo Y, et al. Luteolin Enhances Sarcoplasmic Reticulum Ca2+-ATPase Activity through p38 MAPK Signaling thus Improving Rat Cardiac Function after Ischemia/Reperfusion. Cell Physiol Biochem 2017;41:999-1010.
95. Tufekci KU, Eltutan BI, Isci KB, et al. Resveratrol Inhibits NLRP3 Inflammasome-Induced Pyroptosis and miR-155 Expression in Microglia Through Sirt1/AMPK Pathway. Neurotox Res 2021;39:1812-29.
96. Song P, Shen DF, Meng YY, et al. Geniposide protects

 

against sepsis-induced myocardial dysfunction through AMPKα-dependent pathway. Free Radic Biol Med 2020;152:186-96.
97. Kikuchi S, Piraino G, O'Connor M, et al. Hepatocyte-Specific Deletion of AMPKalpha1 Results in Worse Outcomes in Mice Subjected to Sepsis in a Sex-Specific Manner. Front Immunol 2020;11:210.
98. Patel VB, Mori J, McLean BA, et al. ACE2 Deficiency Worsens Epicardial Adipose Tissue Inflammation and Cardiac Dysfunction in Response to Diet-Induced Obesity. Diabetes 2016;65:85-95.
99. Murça TM, Moraes PL, Capuruço CA, et al. Oral administration of an angiotensin-converting enzyme 2 activator ameliorates diabetes-induced cardiac dysfunction. Regul Pept 2012;177:107-15.
100. Hoffmann M, Kleine-Weber H, Schroeder S, et al. SARS-CoV-2 Cell Entry Depends on ACE2 and TMPRSS2 and Is Blocked by a Clinically Proven Protease Inhibitor. Cell 2020;181:271-80.e8.
101. Monteil V, Kwon H, Prado P, et al. Inhibition of SARS-CoV-2 Infections in Engineered Human Tissues Using Clinical-Grade Soluble Human ACE2. Cell 2020;181:905-13.e7.
102. Smeding L, Plötz FB, Groeneveld AB, et al. Structural changes of the heart during severe sepsis or septic shock. Shock 2012;37:449-56.
103. Willingham SB, Allen IC, Bergstralh DT, et al. NLRP3 (NALP3, Cryopyrin) facilitates in vivo caspase-1 activation, necrosis, and HMGB1 release via inflammasome-dependent and -independent pathways. J Immunol 2009;183:2008-15.
104. Sandanger Ø, Ranheim T, Vinge LE, et al. The NLRP3 inflammasome is up-regulated in cardiac fibroblasts and mediates myocardial ischaemia-reperfusion injury. Cardiovasc Res 2013;99:164-74.
105. Mezzaroma E, Toldo S, Farkas D, et al. The inflammasome promotes adverse cardiac remodeling following acute myocardial infarction in the mouse. Proc Natl Acad Sci U S A 2011;108:19725-30.
106. Liu Y, Lian K, Zhang L, et al. TXNIP mediates NLRP3 inflammasome activation in cardiac microvascular endothelial cells as a novel mechanism in myocardial ischemia/reperfusion injury. Basic Res Cardiol 2014;109:415.
107. Dugar SP, Vallabhajosyula S. Right ventricle in sepsis: clinical and research priority. Heart 2020;106:1629-30.
108. Vallabhajosyula S, Shankar A, Vojjini R, et al. Impact of Right Ventricular Dysfunction on Short-term and Long-term Mortality in Sepsis: A Meta-analysis of 1,373 Patients. Chest 2021;159:2254-63.

(English Language Editor: J. Jones)

**Cite this article as:** Wu C, Chen Y, Zhou P, Hu Z. Recombinant human angiotensin-converting enzyme 2 plays a protective role in mice with sepsis-induced cardiac dysfunction through multiple signaling pathways dependent on converting angiotensin II to angiotensin 1–7. Ann Transl Med 2023;11(1):13. doi: 10.21037/atm-22-6016

 

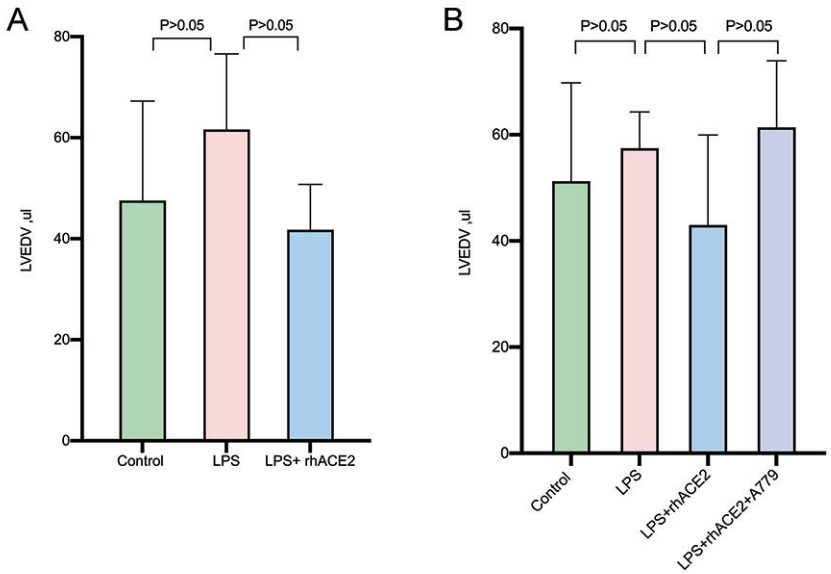


**Figure S1** The LVEDV of mice among groups are comparable. (A) Quantitative analysis of LVEDV among three groups (n=6). (B) Quantitative analysis of LVEDV among four groups (n=6). Data are expressed as mean ± SD. LVEDV, left ventricular end diastolic volume; LPS, lipopolysaccharide; rhACE2, recombinant human angiotensin-converting enzyme 2; SD, standard deviation.

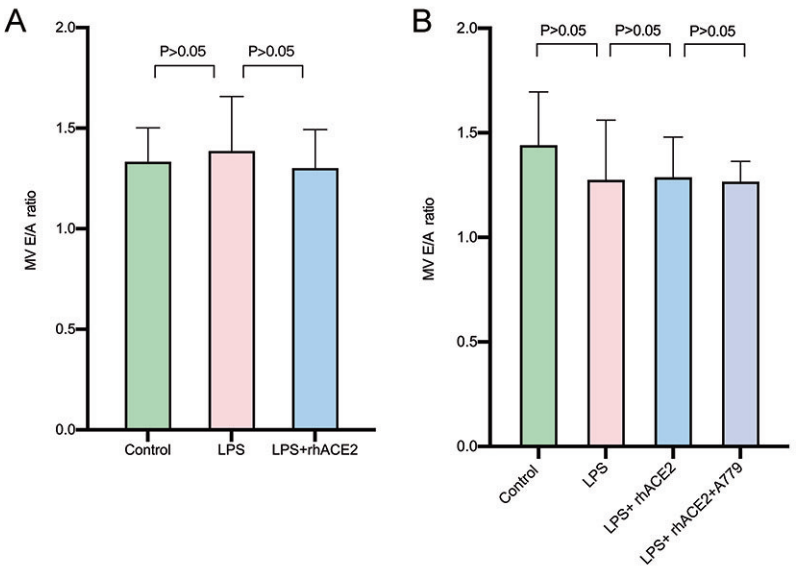


**Figure S2** The MV E/A ratios from mice among groups are comparable. (A) Quantitative analysis of MV E/A ratios among three groups (n=6). (B) Quantitative analysis of MV E/A ratios among four groups (n=6). Data are expressed as mean ± SD. MV E/A ratio, the ratio of the peak velocity of the early filling (E) wave to the atrial contraction (A) wave of mitral inflow; LPS, lipopolysaccharide; rhACE2, recombinant human angiotensin-converting enzyme 2; SD, standard deviation.


https://dx.doi.org/10.21037/atm-22-6016